Localized Internal Gravity Waves Breaking Region and its Implications for Middle Atmospheric Circulation and Stratosphere-Troposphere Exchange

EGU2015-5190
Y284

Petr Sacha[1], Petr Pisoft[1], Friederike Lilienthal[2] and Christoph Jacobi[2]

[1]Department of Atmospheric Physics, Faculty of Mathematics and Physics, Charles University in Prague, Prague, Czech Republic, petr.sacha@mff.cuni.cz; [2]Institute for Meteorology, University of Leipzig, Stephanstr. 3, D-04103 Leipzig, Germany

Abstract: The Internal gravity waves are widely recognized to contribute significantly to the energy and angular momentum transport. They play significant role in affecting many of the middle atmospheric phenomena (like QBO or Brewer-Dobson circulation). Using the GPS RO density profiles, we have discovered a localized area of enhanced IGW activity and breaking in the lower stratosphere of Eastern Asia/North-western Pacific region. Using a mechanistic model for the middle atmosphere, 3D EP flux and residual circulation diagnostics, we investigate longitudinal variability of the Brewer-Dobson circulation and a hypothesis of its enhanced branch in this region. Further, we study possible formation and propagation directions of planetary waves caused by such a localized forcing and discuss the consequences for the stratosphere-troposphere exchange and polar vortex stability.

Background

- Anomalous area of small annual cycle amplitude located across the Northern Pacific and Eastern Asia extending vertically from about 50 hPa up to 10 hPa revealed using the pseudo-2D wavelet transform (see Fig. 2) analysis of MERRA reanalyzed climatology series.
- Closer look at the climatology distribution of temperature, zonal wind and ozone fields (see Fig. 4)
  - Region of the highest temperatures in the Northern Hemisphere in autumn and winter.
  - Jet shifted northward above our area gaining a wave-1 pattern, rapid deceleration starting in our region and continuing above Pacific.
  - Ozone concentration fields also shifted northward having a wave-1 pattern in Winter while showing NH maxima in autumn and spring.

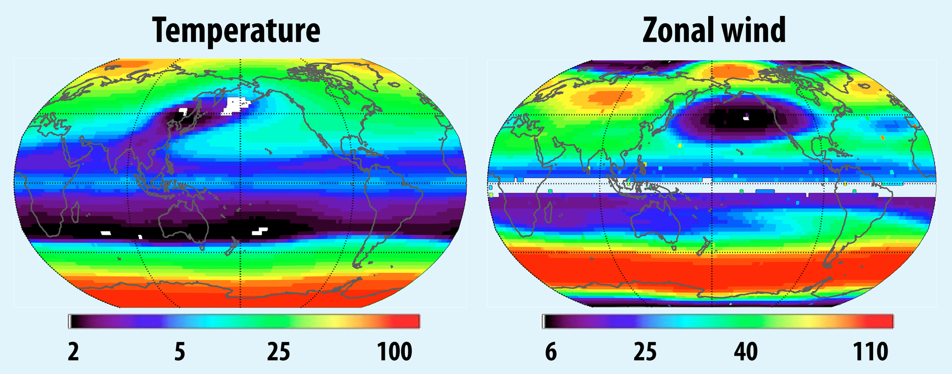

Figure 2: Annual cycle amplitudes in the temperature (left) and zonal wind (right) series at 30 hPa. The color-scale used represents square root of the wavelet power in K for temperature and in m/s for zonal wind.

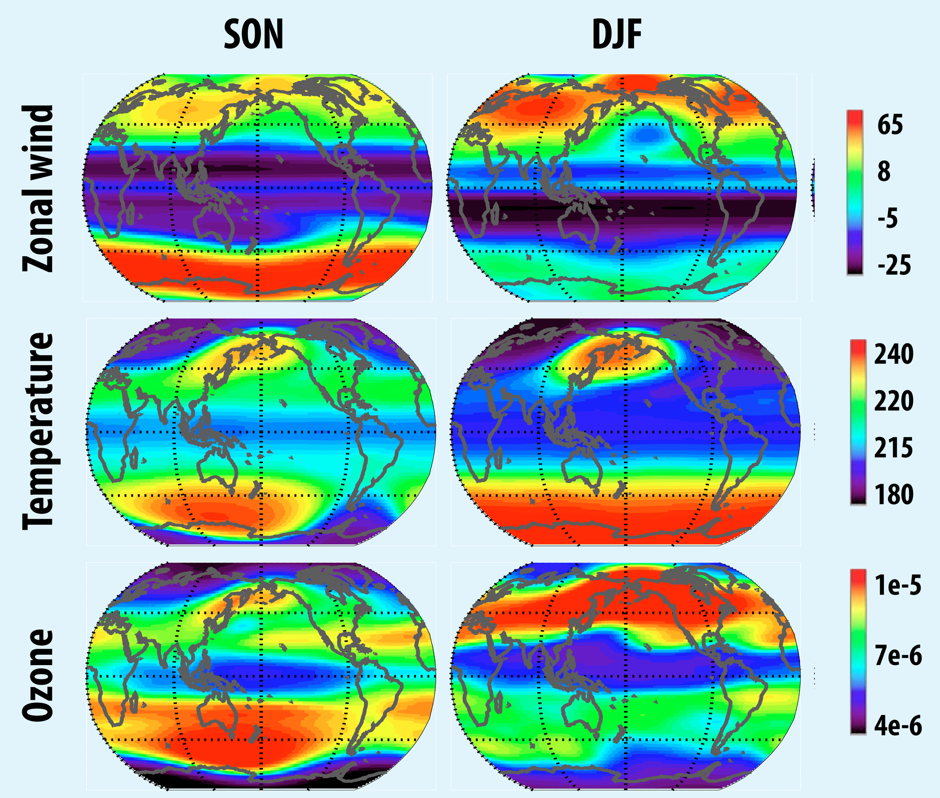

Figure 3: Seasonal averages in zonal wind in m/s, temperature in K and ozone mass mixing ratio in mg/kg at 30 hPa for 1979-2013 time period using MERRA series.

Methodology

- L2 level FORMOSAT-3/COSMIC data on a 3° × 3° grid from 2007 to 2010. GPS RO density profiles (Šácha et al., 2014) from tropopause to 35 m (Fig. 1).
- The potential energy density of disturbances per unit mass (Ep) as a proxy for IGW activity

$$Ep = \frac{1}{2}N^2\langle\xi^2\rangle = \frac{1}{2}\left(\frac{g}{N}\right)^2\left\langle\left(\frac{\rho'}{\rho_0}\right)^2\right\rangle$$

- To access the stability of the wave field:
  - Dynamical instability gradient Richardson number

$$Ri_g = \frac{g^2}{N^4}\left\langle\left[\frac{\partial}{\partial z}\left(\frac{\rho'}{\rho_0}\right)\right]^2\right\rangle$$

  - Rayleigh-Taylor convective instability maximum growth rate of disturbances.

$$\sigma^2 = \frac{g}{\rho_0}\left(\frac{d\bar{\rho}}{dz} + \frac{\partial\rho'}{\partial z}\right)$$

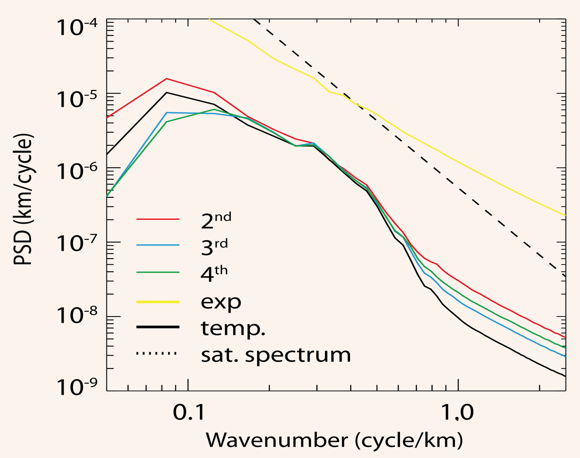

Figure 1. Vertical wavenumber power spectral density for the normalized density perturbations from different backgrounds and temperature normalized perturbations compared with the theoretical saturated spectra.

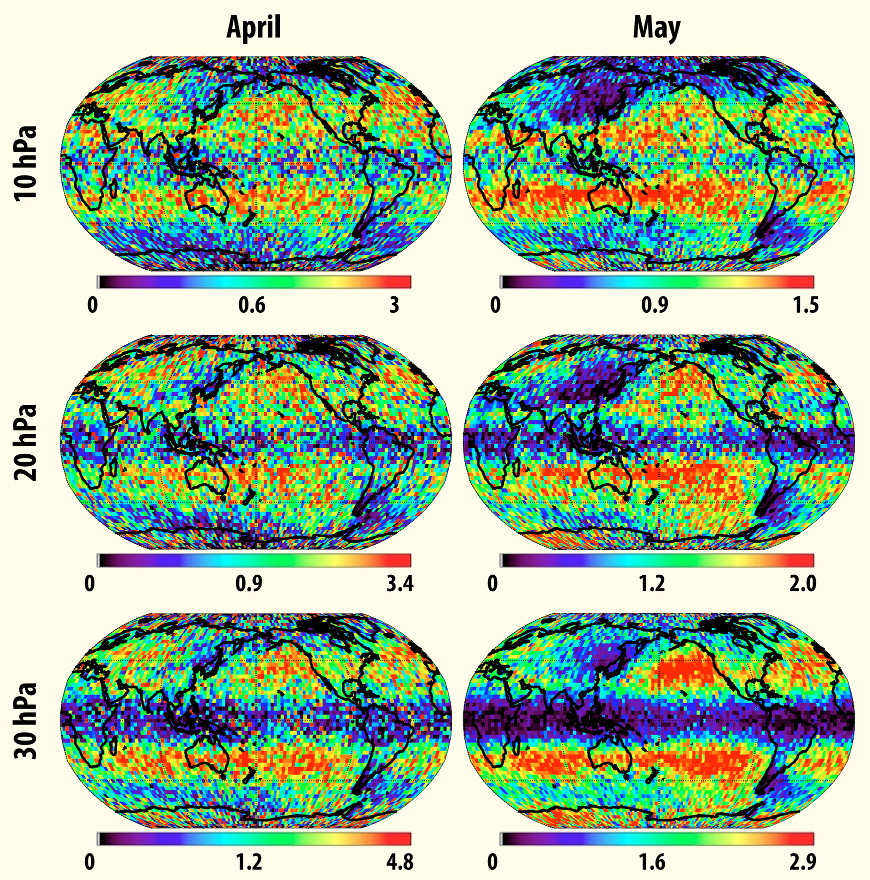

Figure 5. Selected monthly means of the gradient Richardson number at 10, 20 and 30 hPa.

Results I

Analysis of geographical and seasonal distribution of IGW activity and effects

- Distribution of potential energy of disturbances: In average, a distinguished region of high IGW activity and of maximal values in the Northern Hemisphere in October and November (see Figure 4). This area is significant starting from the 70 hPa level up to the 6 hPa level.
- Wave breaking indication: Richardson number and convective instability growth rate values and distributions are further accentuating the importance of our area making it a dominant feature of the maps across all the levels even in spring and winter months and being suggestive of vertically robust and long lasting breaking of IGWs (See Figures 5 and 6).
- Possible wave sources
  - Convective activity connected with the Kuroshio current in autumn.
  - Low values of cumulative wind rotation above our region are favorable for vertical propagation of orographic waves (c_p=0).
  - Surface winds suggestive of orographic creation of IGW due to the topography of Japan, Sacha lin, Korean Peninsula and eastern Asia coastline.
  - In situ wave generation in the upper troposphere/lower stratosphere (Mohri (1953) – subtropical and polar jet stream merging)

Why not discovered before?

- best visibility in autumn
- proper visualization approach
- density profiles
- Ep is inappropriate wave activity proxy (Fig 1)

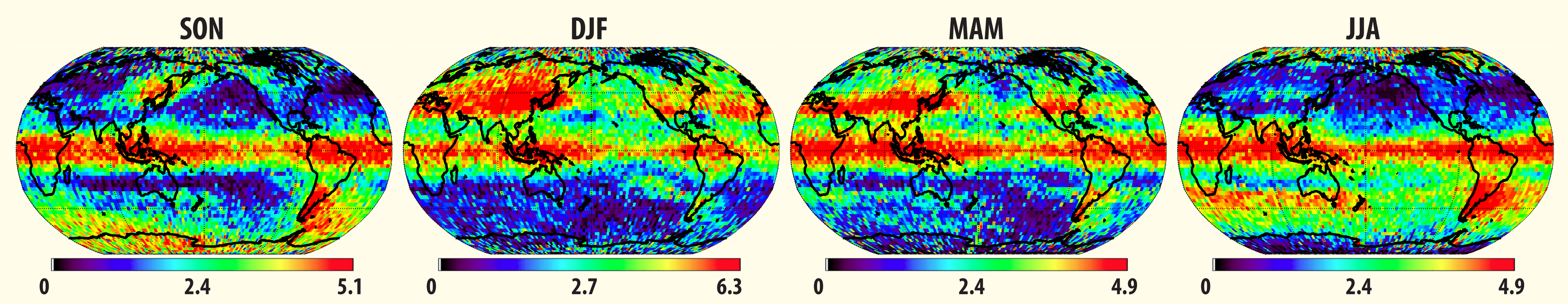

Figure 4. Seasonal means of the potential energy in J/kg averaged across the whole vertical profile for the studied time period 2007-2010.

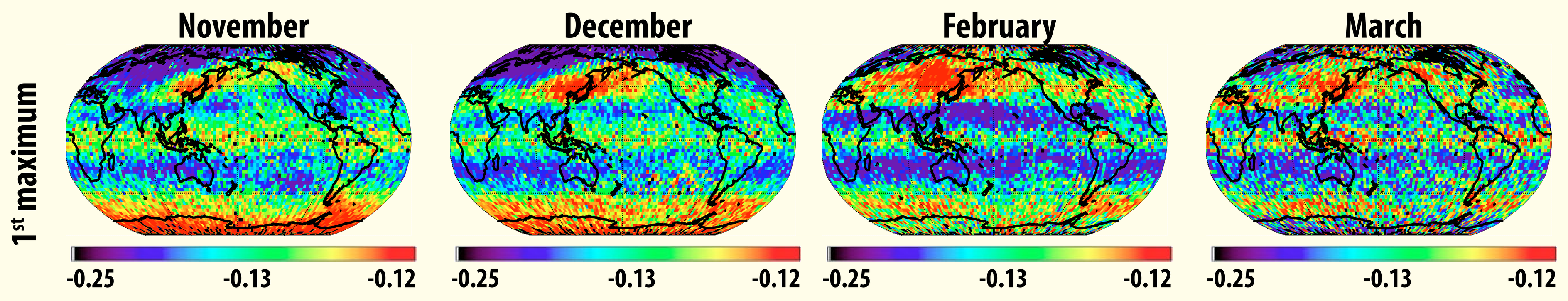

Figure 6. Selected monthly means of selected (secondary) sigma maxima in s^{-2} for the studied time period 2007-2010.

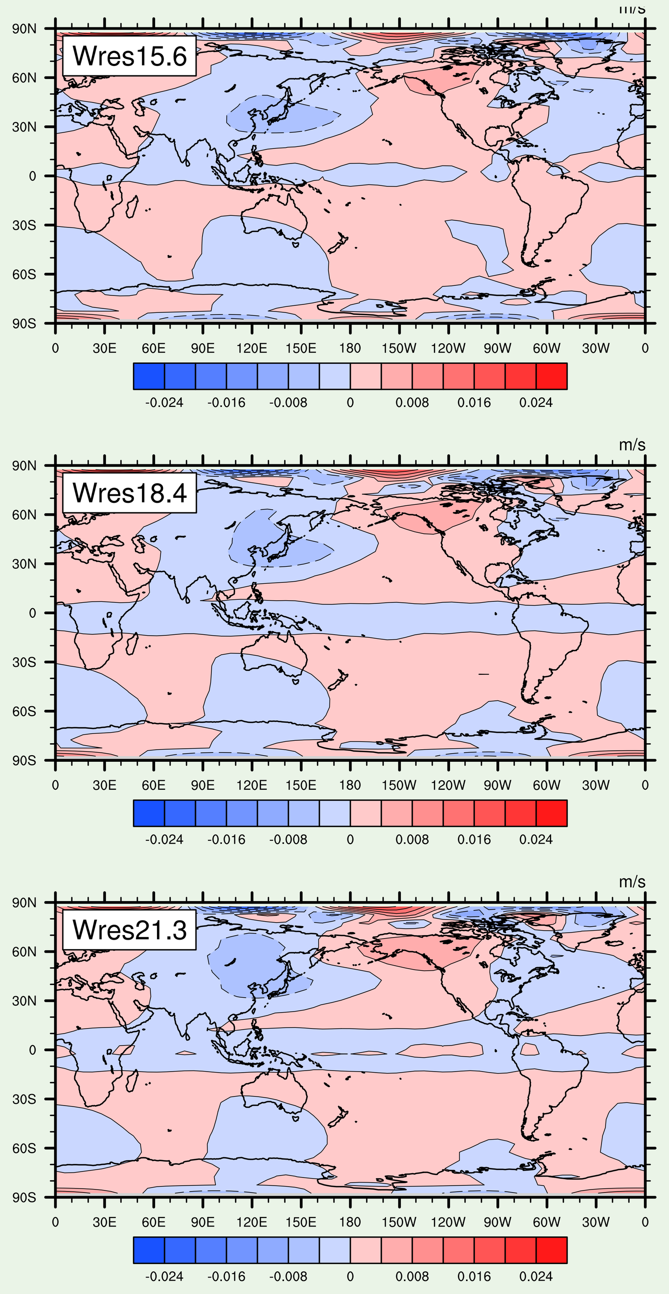

Figure 8. Geographical distribution of the residual vertical velocity (Kinoshita and Sato, 2013) on three consequent model levels in the LS region

Results II

Longitudinal variability of BDC and planetary waves sourcing

- MUAM 3D mechanistic circulation model (Pogoreltsev et al., 2007) runs with IGW parameterization input based on geographical distribution of wave activity from GPS RO.
- In comparison with the reference run for January – 2D Eliassen-Palm flux analysis reveals in the LS stronger planetary wave propagation from midlatitudes equatorward and at the edge of polar vortex (Fig. 7).
- 3D analysis reveals enhanced downwelling above NP/EA region penetrating to lower levels than elsewhere.

EPflux and differences between runs

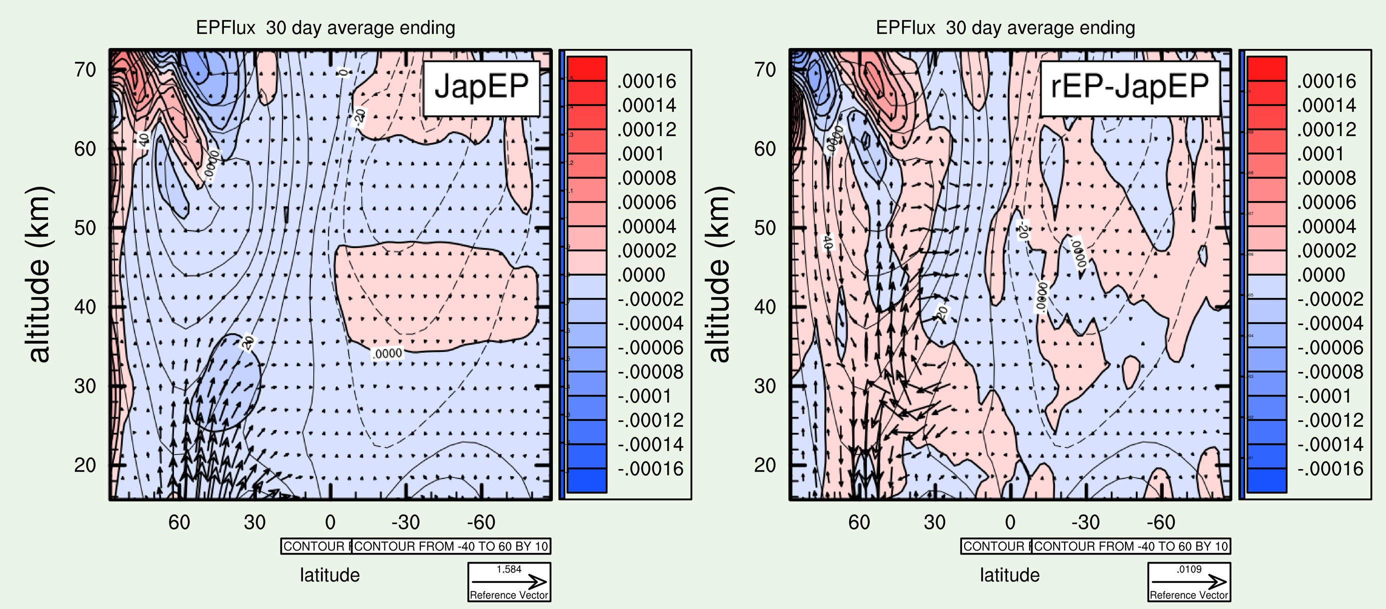

Figure 7. Left: Mean E-P flux and its divergence from GPS RO based IGW weights run for January conditions, contours show mean zonal wind. Right: Difference between reference and GPS RO based run.

Summary and conclusions

- Region of low annual cycle amplitude, highest temperatures in the NH stratosphere in autumn and winter (MERRA reanalysis).
- Using GPS RO data high IGW potential energy values were find. Static and dynamic stability indicators suggestive of massive wave breaking in this region (Submitted to ACP).
- 2D E-P flux diagnostics of MUAM runs reveals enhanced equatorward and poleward propagation of planetary waves, if the IGW hotspot area is included – possible consequences for STE and vortex dynamics.
- Distributions of atmospheric quantities, ozone concentrations (MERRA) and 3D analysis of MUAM runs are pointing to robust downwelling of equatorial air masses (enhanced branch of Brewer-Dobson circulation) reaching deeper in the stratosphere than elsewhere. The causality is unclear - product of wave mean flow interactions and induced residual circulation in 3D.

REFERENCES:
Demirhan Bari, D., Gabriel, A., Körnich, H., & Peters, D. W. H. (2013). The effect of zonal asymmetries in the Brewer-Dobson circulation on ozone and water vapor distributions in the northern middle atmosphere. Journal of Geophysical Research: Atmospheres, 118(9), 3447-3466.
Ern, M., Preusse, P., Gille, J. C., Hepplewhite, C. L., Mlynczak, M. G., Russell, J. M., and Riese, M.: Implications for atmospheric dynamics derived from global observations of gravity wave momentum flux in stratosphere and mesosphere, J. Geophys. Res.-Atmos., 116, D19107, doi:10.1029/2011JD015821, 2011.
Garcia, R. R. and Randel,W. J.: Acceleration of the Brewer-Dobson circulation due to increases in greenhouse gases, J. Atmos. Sci., 65, 2731–2739, 2008.
Kinoshita, T., & Sato, K. (2013). A Formulation of Three-Dimensional Residual Mean Flow Applicable Both to Inertia–Gravity Waves and to Rossby Waves. Journal of the Atmospheric Sciences, 70(6), 1577-1602.
Marshall, A. G. and Scaife, A. A.: Impact of the QBO on surface winter climate, J. Geophys. Res.-Atmos., 114, D18110, doi:10.1029/2009JD011737, 2009.
McDonald, A. J., B. Tan, and X. Chu (2010), Role of gravity waves in the spatial and temporal variability of stratospheric temperature measured by COSMIC/FORMOSAT3 and Rayleigh lidar observations, J. Geophys. Res., 115, D19128, doi:10.1029/2009JD013658.
Šácha, P., Foelsche, U., & Pišoft, P. (2014). Atmos. Meas. Tech., 7, 4123-4132, doi:10.5194/amt-7-4123-2014, 2014.
Senft, D. C., & Gardner, C. S. (1991). Seasonal variability of gravity wave activity and spectra in the mesopause region at Urbana. Journal of Geophysical Research: Atmospheres (1984–2012), 96(D9), 17229-17264.
Wilson, R., Chanin, M. L., & Hauchecorne, A. (1991). Gravity waves in the middle atmosphere observed by Rayleigh lidar: 2. Climatology. Journal of Geophysical Research: Atmospheres (1984–2012), 96(D3), 5169-5183.

ACKNOWLEDGEMENTS.:
The study was supported by the Charles University in Prague, project GA
UK No 108313, by the Aktion program, by the grant no. SVV-2014-26096, and by the Austrian Science Fund (FWF; BENCHCLIM project P22293-N21. UCAR/CDAAC (Boulder, CO, USA) is acknowledged for the provision RO data.
Finally we thank Andrea K. Steiner (WEGC, University of Graz) for fruitful discussions.